JOURNAL OF SOLID STATE CHEMISTRY **140,** 331–336 (1998)
ARTICLE NO. SC987895

Structural and Morphological Changes Associated with Charge Ordering in $La_{0.2}Ca_{0.8}MnO_3$

Y. Murakami,* D. Shindo,* H. Chiba,† M. Kikuchi,† and Y. Syono†

*Institute for Advanced Materials Processing, Tohoku University, Katahira, Sendai 980-77, Japan; †Institute for Materials Research, Tohoku University, Katahira, Sendai 980-77, Japan

Received January 20, 1998; in revised form May 4, 1998; accepted May 7, 1998

Both structural and morphological changes associated with charge ordering in perovskite manganese oxide, $La_{0.2}Ca_{0.8}MnO_3$, were studied by electron microscopic observations with imaging plates. Two types of long-period structures were observed at around 107 K, i.e., the structure with about 4-fold periodicity to the unit lattice distance of the room-temperature phase and the structure with much larger periodicity such as 23-fold. These long-period structures were suggested to be formed by a similar mechanism due to charge ordering of manganese ions, since they showed some crystallographic and morphological similarities. Superlattice reflections of a near 4-fold structure were observed as a function of temperature. They were found to become weak diffuse scattering just before the disappearance, and the peak positions moved slightly with heating. Considering those features, the kinetics of the charge ordering in this oxide was discussed. © 1998 Academic Press

1. INTRODUCTION

Perovskite manganese oxides have acquired great interest due to their unique behaviors such as colossal magnetoresistance (1–3) and magnetic-field-induced structural transformation (4) etc. Charge ordering of manganese ions (5–10), which is observed in the oxides in a specific composition range, is another interesting phenomenon. In those perovskite oxides, e_g (Mn3d) electrons become less mobile below the critical temperature T_{CO}, and the manganese ions take two possible states, such as Mn^{3+} and Mn^{4+}. Because of the Coulomb interaction, the two types of manganese ions are periodically distributed in the crystal below T_{CO}. The charge ordering in perovskite manganese oxides was actually observed by a conventional electron diffraction method (7–10) as the appearance of superlattice reflections.

Observable structures in the charge-ordered state are thought to be related to the magnetic structure below T_{CO}, and this is dependent on the charge-composition ratio between the manganese ions (i.e., Mn^{3+}/Mn^{4+} ratio) in a specimen. This charge-composition ratio can be controlled by changing the specimen composition. For example, in the case of $La_{1-x}Ca_xMnO_3$, the Mn^{3+}/Mn^{4+} ratio tends to increase with decreasing Ca content. However, detailed electron microscopic observations of charge ordering, where both the morphological and structural changes were carefully studied, have been carried out for the oxide with composition $x \approx 0.5$, i.e., the oxide showing the CE-type antiferromagnetic structure.

Meanwhile, the present authors studied charge ordering in $Bi_{0.2}Ca_{0.8}MnO_3$ (11, 12), which lies in a Mn^{4+}-rich composition range and shows the C-type antiferromagnetic structure below T_{CO} (13). They observed two types of long-period structures associated with the charge ordering, i.e., the one with 4-fold periodicity to the unit lattice distance of the parent phase and the one with much larger periodicity, such as 32-fold (14). Although the 4-fold periodicity was thought to be the favorable structure associated with the charge ordering in this oxide, the two types of long-period structures were expected to be closely related because of several similarities in crystallographic and morphological aspects. A charge ordered structure with such large periodicity has not been observed in other perovskite manganese oxides. Thus, further investigations for other systems are required to elucidate the nature of the existing two types of the long-period structure.

The purpose of the present paper is to investigate both structural and morphological changes associated with charge ordering in $La_{0.2}Ca_{0.8}MnO_3$, which lies in a Mn^{4+}-rich composition range as the case of $Bi_{0.2}Ca_{0.8}MnO_3$. Furthermore, the kinetics of the charge ordering in $La_{0.2}Ca_{0.8}MnO_3$ is discussed by observing the associated superlattice reflections as a function of temperature.

2. EXPERIMENTAL PROCEDURES

A $La_{0.2}Ca_{0.8}MnO_3$ pellet was prepared by a conventional ceramics method. The pellet was prefired in air at 1273 K, followed by a second firing in oxygen at 1623 K. It was finally annealed in oxygen at 1123 K to improve

0022-4596/98 $25.00

homogeneity. The oxygen content was determined to be 3.00 by the iodine titration method. The temperature dependence of electric resistance was measured by a conventional four-terminal method. Magnetization vs temperature curves were obtained using a Quantum Design superconducting quantum interference device (SQUID) magnetometer. Specimens for electron microscopic observations were prepared by standard procedures of slicing, mechanical polishing, and ion-milling. Structural and morphological changes in $La_{0.2}Ca_{0.8}MnO_3$ upon cooling were observed by using JEM-2010 and JEM-2000EX electron microscopes employing cooling specimen holders. Both electron microscopic images and diffraction patterns were measured using imaging plates (Fuji FDL-URV) (15, 16).

3. RESULTS AND DISCUSSION

3.1. Structural and Morphological Changes with Charge Ordering

Both electric resistance and magnetization in $La_{0.2}Ca_{0.8}MnO_3$ were measured as a function of temperature and the result was shown in Fig. 1. The temperature dependence was quite similar to that of $Bi_{0.2}Ca_{0.8}MnO_3$ (11), but the critical temperature T_{CO} of $La_{0.2}Ca_{0.8}MnO_3$ ($T_{CO} = 195$ K) was about 35 K higher than that of $Bi_{0.2}Ca_{0.8}MnO_3$. In a temperature range between 350 K and T_{CO}, the magnetization increases monotonically with decreasing temperature, and this oxide is thought to exhibit weak ferromagnetism due to double exchange interaction (12). No appreciable change in the electric resistance was observed in this temperature range. However, below the critical temperature T_{CO}, the magnetization was reduced with cooling being accompanied by a significant increase of the electric resistance. The resistivity at 40 K, for example, was more than 10^4 times larger than that at room temperature, although the metallic state was not achieved. An anomaly in the magnetization curve was also found at around 100 K. This effect, which was observed below T_{CO}, is thought to be due to the magnetic transformation to the antiferromagnetic state as observed in $Bi_{0.2}Ca_{0.8}MnO_3$ (11,13,14). Bao *et al.* (13) mentioned that the deviation between T_{CO} and magnetic transformation temperature (T_N) was essential in perovskite manganese oxides exhibiting charge ordering. If we consider those features, which are consistent with those of other systems exhibiting charge ordering (9, 10, 13, 17, 18), the $La_{0.2}Ca_{0.8}MnO_3$ is thought to exhibit charge ordering below $T_{CO} = 195$ K.

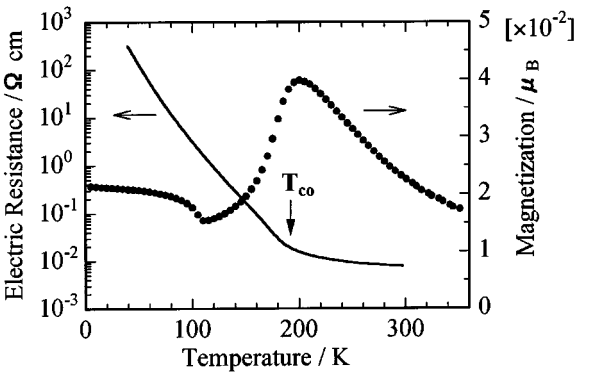

FIG. 1. Electric resistance and magnetization in $La_{0.2}Ca_{0.8}MnO_3$ as a function of temperature.

Both the morphology and the structure of $La_{0.2}Ca_{0.8}MnO_3$ were investigated above and below the critical temperature T_{CO} using an electron microscope. Figure 2a shows a typical electron microscopic image of this oxide taken at 293 K ($> T_{CO}$), in which a noticeable fine structure is not visible. The diffraction pattern observed at this temperature (Fig. 2b) was indexed by taking an orthorhombic structure[1] with the lattice correspondence $a \sim \sqrt{2}a_c$, $b \sim \sqrt{2}a_c$ and $c \sim 2a_c$, where a_c represents the lattice constant of the simple perovskite (cubic) structure, although the orthorhombic distortion was quite small.

When the specimen was cooled to 107 K, two types of bandlike morphology appeared. We first recognize a bandlike morphology consisting of wide plates as indicated by "A" and "B" in Fig. 2c, whose bandwidth was about 12 nm. The morphology was constructed from two variants (i.e., "A" and "B," variants of the *low temperature phase*), each of which was plate perpendicular to the a^* and b^* axes of the parent phase, respectively. This morphological change was accompanied by a structural change as in the following. If we compare the diffraction pattern in Fig. 2b (293 K) with that of Fig. 2d (107 K), we notice that the lattice parameter does change greatly even by cooling to a temperature below T_{CO}. (Thus the diffraction pattern of Fig. 2d was indexed by taking the unit cell of the parent phase.) However, we find existing superlattice reflections along the a^* and b^* axes in Fig. 2d, while they are absent in Fig. 2b. The presence of those superlattice reflections is more clearly seen from Fig. 2e, which is an enlarged picture of the enclosed area in Fig. 2d. The superlattice peak positions were determined using an imaging plate, and they were found to be located at around 1/23 positions between fundamental reflections. This value corresponds to the period of 12 nm in a real space, which is consistent with the bandwidth measured in Fig. 2c. Thus, the observed morphology was found to be

[1]There are extra reflections arising from other variants of the *parent phase* as indicated by arrows, since they were smaller than the aperture diameter of the microscope, although they are not clearly seen from Fig. 2a. However, presence of those variants was easily ascertained by a small shift of the aperture position from the central region in Fig. 2a, by which one set of the extra reflections disappeared. A shift to a different direction eliminated another set of the extra reflections. Those extra reflections could be indexed by considering the above orthorhombic structure (i.e., 00*l* reflection of the other variant, etc.).

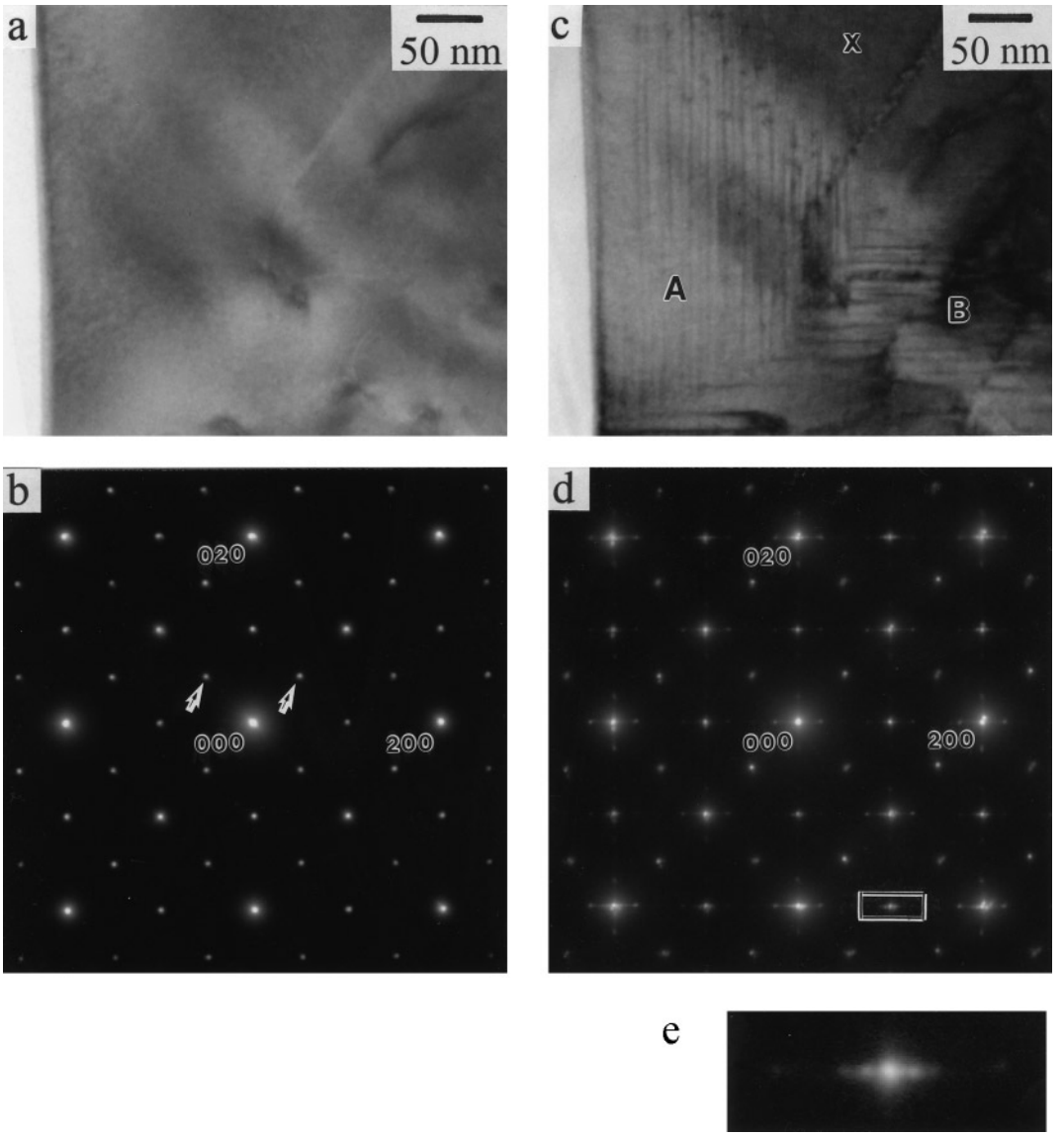

FIG. 2. (a) Typical electron microscopic image and (b) diffraction pattern of $La_{0.2}Ca_{0.8}MnO_3$ at 293 K (above the critical temperature T_{CO}). Both (c) morphological and (d) structural changes were observed by cooling the specimen down to 107 K (below T_{CO}). Letters "A" and "B" represent variants of the low temperature phase. Another type of bandlike morphology, which consists of narrower bands compared with those in "A" and "B", is present around "X" as represented in Fig. 3. (e) Enlarged picture for the enclosed area in diffraction pattern of (d) in which superlattice reflections along the a^* axis are visible.

a long-period structure, whose periodicity was quite large, about 23-fold to the unit lattice distance of the parent phase.

Another type of a long-period structure was observed below T_{CO} as shown in Fig. 3a, which is an enlarged image of the area around "X" in Fig. 2c. In this region, a bandlike morphology with much smaller periodicity was present, and the bandwidth was measured to be about 2 nm. Those narrow bands were perpendicular to the a^* axis of the parent phase. (It should be noted that there were also two variants in this narrow bandlike morphology, i.e., those perpendicular to the a^* and b^* axes, as the case of the wider bandlike morphology, although more clearly observed one was solely represented in Fig. 3a. The presence of the two variants was also ascertained by analyzing a diffraction pattern.) Figure 3b shows a diffraction pattern obtained from the area around "X" in Fig. 2c. We recognize superlattice reflections existing at around 1/4 positions between fundamental reflections, as consistent with the bandwidth in Fig. 3a. Thus, another type of bandlike morphology was shown to be a long-period structure with about 4-fold periodicity to the unit lattice distance of the parent phase.

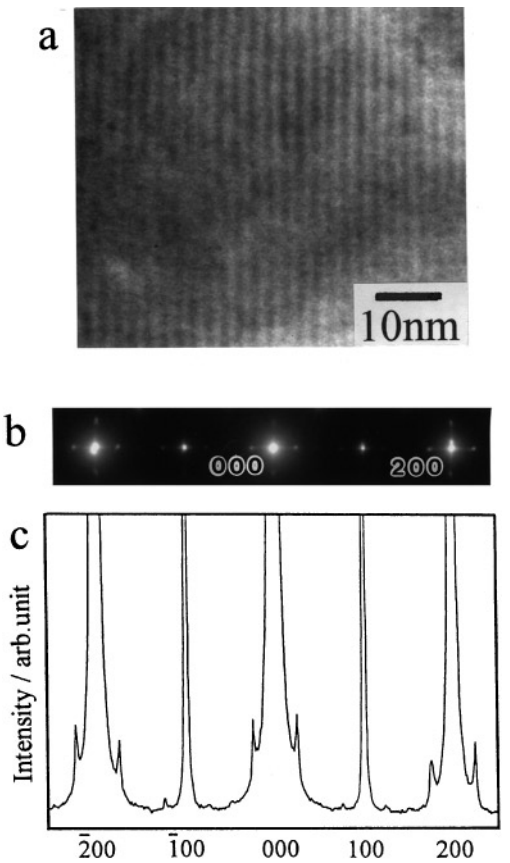

FIG. 3. (a) Enlarged picture for the area around "X" in Fig. 2c, where another band-like morphology consisting of narrower bands is visible. (b) Diffraction pattern obtained from the area around "X" in Fig. 2c. (c) Intensity profile along the a^* axis for the superlattice reflections in (b).

Superlattice peak positions were somewhat different depending on observed domains and specimens (peak position, 0.23–0.25). Periodicity of the other type of the long-period structure (i.e., with wider bands) was also dependent on observed regions, but the period was still much larger than that of the 4-fold one.

The two types of long-period structure have some common morphological and crystallographic features, as in the following. Both of them showed a characteristic bandlike morphology consisting of two variants with the orientation relationship $[100]_{V1}//[010]_{V2}$, $[010]_{V1}//[\bar{1}00]_{V2}$, and $[001]_{V1}//[001]_{V2}$, where V1 and V2 denote the two variants of the *low temperature phase*. The two variants were created in a single crystal region of the parent phase with cooling, but they disappeared by a subsequent heating to a temperature above T_{CO} and the original single crystal region of the parent phase was regained. This point indicates that those structural transformations are crystallographically reversible. It seems that only one considerable difference between the two types of long-period structures lies in the periodicity. If we consider those points, we can interpret that the two types of long-period structures are closely related to each other and created by a similar mechanism. Thus, the origin of the structural transformations is further discussed with a near 4-fold structure. The observed structural phase transformation is expected to be attributed to the charge ordering if we consider the temperature dependence of both electric resistance and magnetization in Fig. 1. Direct observation of charge ordering seems to be difficult by a diffraction technique, as far as small difference of the atomic scattering factors between Mn^{3+} and Mn^{4+} ions are considered. However, since charge ordering results in an appreciable strain around Mn^{3+} ions due to the Jahn–Teller effect, the observation by diffraction will be possible as detection of the static strain. As is well known, static strain in a crystal produces characteristic intensity distribution in a diffraction pattern, where the associated superlattice reflections or diffuse scattering show the intensity maximum at a certain position apart from the origin in a reciprocal lattice space (19, 20). Considering this point, an intensity profile was obtained from the diffraction pattern in Fig. 3b, and the result was shown in Fig. 3c. It was found that the intensity of the superlattice reflections was asymmetric around the fundamental reflections, where the one in a higher angle was stronger than that in a lower angle (e.g., see superlattice reflections around the 200 reflection). This feature is quite consistent with the case of existing static strain. Thus, occurrence of charge ordering in $La_{0.2}Ca_{0.8}MnO_3$ was confirmed by an electron diffraction based on a precise analysis with an imaging plate.

As briefly mentioned in the previous section, detailed electron microscopic observations of charge ordering in $La_{1-x}Ca_xMnO_3$, where both the morphological and structural changes were discussed, have been carried out for the oxide with composition x around 0.5, i.e., the one exhibiting the CE-type antiferromagnetic structure (9). The present specimen is distinct from the previous one in the following respects; it belongs to the Mn^{4+}-rich composition range ($x > 0.5$), and its Mn^{4+} content is thought to be much higher than the Mn^{3+} content (probably, $Mn^{3+}/Mn^{4+} \approx 14$). In the present specimen, two types of long-period structures were observed as a result of charge ordering, i.e., the nearly 4-fold structure and the one with much larger periodicity such as 23-fold. It is expected that this specimen shows the C-type antiferromagnetic structure below T_{CO}, as far as the previous reports for the manganese oxides with similar charge–composition ratio are taken into consideration (5, 6, 12–14). If we consider this point, the favorable structure associated with charge ordering in $La_{0.2}Ca_{0.8}MnO_3$ is thought to be the near 4-fold structure rather than the one with much larger periodicity such as 23-fold.

Two types of long-period structures were also observed in $Bi_{0.2}Ca_{0.8}MnO_3$ (14), where the charge–composition ratio

(the Mn^{3+}/Mn^{4+} ratio) was thought to be close to the present one. Although the critical temperature T_{CO}, which is a measure of stability of the charge ordered state, was higher in $La_{0.2}Ca_{0.8}MnO_3$ than that in $Bi_{0.2}Ca_{0.8}MnO_3$ (12), the low temperature phases in those oxides showed some common crystallographic and morphological features, e.g., the domain structure consisting of plates perpendicular to the a^* and b^* axes of the parent phase and the combination of two particular variants with the same orientation relationship. Thus, it seems that the mechanisms of charge ordering are similar between those oxides from a crystallographic viewpoint. The two types of long-period structure with charge ordering were also observed in powder specimens (i.e., crushed ones from ceramic ingots) in $Bi_{0.2}Ca_{0.8}MnO_3$ by electron diffraction, which represents that appearance of the two types of long-period structures is not a peculiar event observed in a thin-foiled specimen alone. If we consider those points, we expect that the charge–composition ratio in those oxides, where the content of Mn^{4+} ions is much larger than that of Mn^{3+} ions, is responsible for the formation of two types of long-period structures. As mentioned before, a favorable structure associated with charge ordering in $La_{0.2}Ca_{0.8}MnO_3$ is expected to be the near 4-fold structure rather than the one with much larger periodicity. However, in this oxide, the near 4-fold structure will not be created in the entire volume of the specimen because of the compositional restriction; i.e., we expect that the 4-fold periodicity can be realized by a regular arrangement of one Mn^{3+} ion plus three Mn^{4+} ions, while the charge–composition ratio in this specimen (averaged value) is about $Mn^{3+}/Mn^{4+} \approx 1/4$. Under this circumstance, charge ordering may be achieved with different periodicity surrounding the favorable 4-fold structure. Although a quite large periodicity such as 23-fold was observed in a domain around the near 4-fold structure, this is not thought to be the unique structure in the wide bandlike morphology. In fact, in $Bi_{0.2}Ca_{0.8}MnO_3$, some different periodicities such as 32-fold and 36-fold were simultaneously observed around the 4-fold structure. In contrast, periodicity in the narrow band-like morphology was close to the 4-fold one. Those points will be another ground to suggest that the near 4-fold structure is a favored charge ordered structure over the ones with much larger periodicity such as 23-fold. To elucidate the formation of the two types of long-period structures with the charge ordering and to make a more precise comparison between those crystal structures, accurate structure analyses are now in progress, where electron diffraction patterns obtained from each structure with imaging plates are analyzed with the support of a computer simulation technique. This point will be discussed in detail in a forthcoming paper. Despite the fact, it was confirmed that charged ordered structures with different periodicity appeared in $La_{0.2}Ca_{0.8}MnO_3$ as the case of $Bi_{0.2}Ca_{0.8}MnO_3$.

3.2. *Kinetics of Charge Ordering in $La_{0.2}Ca_{0.8}MnO_3$*

To discuss kinetics of the charge ordering in $La_{0.2}Ca_{0.8}MnO_3$, superlattice reflections of a nearly 4-fold structure was observed as a function of temperature (Fig. 4). The peak positions were measured to be about 0.23 between fundamental reflections at 107 K. At this temperature, which was much lower than T_{CO}, superlattice reflections in addition to the 200 fundamental reflection were clearly observed (Fig. 4a). We notice from the peak profile that intensity of the superlattice reflection in a higher angle is stronger than that in a lower angle, as consistent with the previous description. (The fundamental reflection slightly splits along the vertical direction because of other variants surrounding the aimed one, i.e., the size of variants was smaller than the aperture diameter of the microscope. However, this effect does not affect the following analysis, where solely peak position and intensity of the superlattice reflections arising from the aimed variant are discussed.) When the specimen was heated, the intensity of the superlattice reflections was weakened. However, the reflection in a higher angle was still stronger than that in a lower angle, as shown in Fig. 4b. This

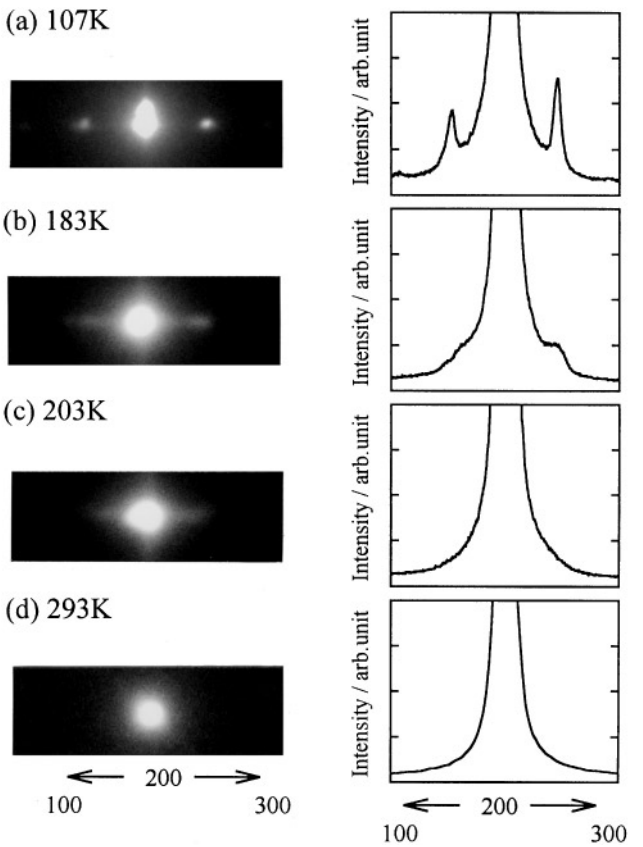

FIG. 4. Temperature dependence of the superlattice reflections associated with charge ordering in $La_{0.2}Ca_{0.8}MnO_3$ (observed for the charge ordered structure with about 4-fold periodicity to the unit lattice distance). See text for details.

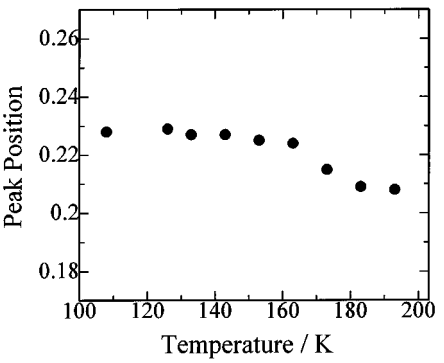

FIG. 5. Temperature dependence of the superlattice peak position in Fig. 4. See text for details.

represents that a charge ordered structure still exists at this temperature. With further heating, the superlattice reflections became weak diffuse scattering along the a^* axis of the parent phase, where observable peaks were absent (Fig. 4c). This diffuse scattering completely disappeared by heating to a higher temperature, and fundamental reflections of the parent phase alone remained, as shown in Fig. 4d.

The intensity decrease of the superlattice reflections indicates that volume of the low temperature phase (charge ordered phase) is reduced with the heating operation. Now, if this oxide exhibits a typical first order phase transformation, there will be such a temperature range where both the parent phase and the low temperature phase coexist. The volume of the low temperature phase will be reduced with heating, but the crystal structure will remain unchanged until this phase completely disappears in the case of a typical first order transformation. In such a case, it is expected that the associated superlattice reflections will not change their peak position until the reverse transformation finishes, and the weak superlattice reflections may still be observable even at a temperature close to T_{CO} without a diffuse scattering state as shown in Fig. 4c. Figure 5 shows a peak position of the superlattice reflections in Fig. 4, which was plotted as a function of temperature (with heating operation). In a temperature range below 163 K, the peak position remained unchanged, and a significant decrease of the peak intensity was not observed. However, above this temperature, a slight change in the peak position occurred with heating accompanied by a considerable decrease of the intensity. (The peak was observable below 193 K, but it could not be observed above this temperature because the superlattice reflection completely became diffuse scattering as shown in Fig. 4.) A shift of the superlattice peak position with increasing temperature was also observed in the charge ordered state of $La_{0.5}Ca_{0.5}MnO_3$ (9), i.e., the oxide exhibiting CE-type antiferromagnetic structure. Thus, this effect is thought to be an essential phenomenon associated with charge ordering. Although charge ordering in the manganese oxides has been explained to be a first order transformation, some features, which are different from the ones expected for a typical first order transformation, were observed as shown in Figs. 4 and 5. As one possible interpretation for this behavior, it is speculated that the periodic arrangement of the manganese ions in the low temperature phase is no longer perfect in this temperature range, i.e., the charge-ordered structure will change into some modulated lattice state before it transforms to the parent phase. Further investigation of the transformation mechanism is in progress and will be discussed in a forthcoming paper.

ACKNOWLEDGMENT

This work was supported by a Grant-in-Aid for Scientific Research on Priority Area and for Encouragement of Young Scientists (Y.M.) from the Ministry of Education, Science and Culture of Japan.

REFERENCES

1. R. von Helmolt, J. Wecker, B. Holzapfel, M. Schultz, and K. Samwer, *Phys. Rev. Lett.* **71,** 2231 (1993).
2. S. Jin, T. H. Tiefel, M. McCormack, R. A. Fastnacht, R. Ramesh, and L. H. Chen, *Science* **264,** 413 (1994).
3. Y. Tomioka, A. Asamitsu, Y. Moritomo, and Y. Tokura, *J. Phys. Soc. Jpn.* **64,** 3626 (1995).
4. P. Schiffer, A. P. Ramirez, W. Bao, and S.-W. Cheong, *Phys. Rev. Lett.* **75,** 3336 (1995).
5. E. O. Wollan and W. C. Koehler, *Phys. Rev.* **100,** 545 (1955).
6. J. B. Goodenough, *Phys. Rev.* **100,** 564 (1955).
7. C. H. Chen, S.-W. Cheong, and A. S. Cooper, *Phys. Rev. Lett.* **71,** 2461 (1993).
8. Y. Moritomo, Y. Tomioka, A. Asamitsu, Y. Tokura, and Y. Matsui, *Phys. Rev. B* **51,** 3297 (1995).
9. C. H. Chen, and S.-W. Cheong, *Phys. Rev. Lett.* **76,** 4042 (1996).
10. Ramirez, P. Schiffer, S.-W. Cheong, C. H. Chen, W. Bao, T. T. M. Palstra, P. L. Gammel, D. J. Bishop, and B. Zegarski, *Phys. Rev. Lett.* **76,** 3188 (1996).
11. H. Chiba, M. Kikuchi, K. Kusaba, Y. Muraoka, and Y.Syono, *J. Solid. State Commun.* **99,** 499 (1996).
12. H. Chiba, T. Atou, H. Faqir, M. Kikuchi, and Y. Syono, *Solid State Ionics* **108,** 193 (1998).
13. W. Bao, J. D. Axe, C. H. Chen, and S.-W. Cheong, *Phys. Rev. Lett.* **78,** 543 (1997).
14. Y. Murakami, D. Shindo, H. Chiba, M. Kikuchi, and Y. Syono, *Phys. Rev. B* **55,** 15043 (1997).
15. D. Shindo, T. Oku, J. Kudo, and T. Oikawa, *Ultramicroscopy* **54,** 221 (1994).
16. A. Taniyama, D. Shindo, and T. Oikawa, *J. Electron Microsc.* **16,** 303 (1997).
17. Y. Tomioka, A. Asamitsu, Y. Moritomo, H. Kuwahara, and Y. Tokura, *Phys. Rev. Lett.* **74,** 5108 (1995).
18. H. Kuwahara, Y. Tomioka, A. Asamitsu, Y. Moritomo, and Y. Tokura, *Science* **270,** 961 (1995).
19. J. M. Cowley, "Diffraction Physics." North-Holland P.L., Amsterdam, The Netherlands, 1975.
20. B. J. Sternlieb, J. P. Hill, U. C. Wildgruber, G. M. Luke, B. Nachumi, Y. Moritomo, and Y. Tokura, *Phys. Rev. Lett.* **76,** 2169 (1996).